Colloid Polym Sci (2004) 282: 793–801
DOI 10.1007/s00396-004-1092-5

ORIGINAL CONTRIBUTION

Jeffrey C. Haley
Timothy P. Lodge

Failure of time-temperature superposition in dilute miscible polymer blends

Received: 16 February 2004
Accepted: 4 March 2004
Published online: 30 April 2004

J. C. Haley · T. P. Lodge (✉)
Department of Chemical Engineering and Materials Science, University of Minnesota, Minneapolis MN 55455, USA

T. P. Lodge
Department of Chemistry, University of Minnesota, Minneapolis MN 55455, USA
E-mail: lodge@chem.umn.edu

Abstract The dynamic viscosity for miscible blends of 1,4-polyisoprene and poly(vinyl ethylene) (PVE) at the extremes of composition (1% tracer in 99% matrix) has been measured as a function of temperature. Time-temperature superposition failure is observed in these tracer blends. This observation indicates that intramolecular contributions are crucial in defining the local environment experienced by a polymer segment, as anticipated by self-concentration models. The temperature dependence of the dynamics of the PVE tracer has been extracted, and compared with the model of Lodge and McLeish. The self-concentration effect was found to be even stronger than predicted.

Keywords Time-temperature superposition failure · Dynamic viscosity · 1,4-Polyisoprene · Poly(vinyl ethylene) · Self-concentration models

Introduction

The dynamics of polymeric mixtures are of fundamental importance for the understanding of a wide range of phenomena, including the kinetics of phase separation, the rheological response of block copolymers, and the processing of polymer blends. Of the many different classes of polymer mixtures, binary miscible blends are perhaps the simplest, and thus the most amenable to experimental study. In order to describe the macroscopic rheological response of miscible blends, one must at some point confront the often-complex temperature and composition dependences of the chain dynamics of the blend components.

Miscible polymer blends exhibit several well documented, and initially surprising, phenomena. The empirical time-temperature superposition principle, largely successful for homopolymers, has been shown to fail for several miscible blend systems [1, 2, 3, 4, 5]. The calorimetric glass transition process can be unusually broad in miscible polymer blends [3, 4, 6]. Tracer diffusion measurements have revealed complex composition dependences for individual component dynamics [7, 8, 9]. These observations, along with others, have led to the idea that each blend component experiences its own unique effective glass transition temperature ($T_{g,eff}$) that is composition dependent and differs from the homopolymer glass transition temperatures (T_g) [10].

Two distinct factors are thought to contribute to the difference in $T_{g,eff}$ between blend components. Each blend component retains some intrinsic characteristics in its dynamic behavior. Additionally, each component relaxes in a local environment that is compositionally different from the macroscopic blend. At least three approaches have been employed to describe this compositional heterogeneity. One extends the coupling model [11] in which cooperativity between molecules leads to a broad distribution of local environments, and thus a broad distribution of relaxation times for each component [12, 13]. The second approach stresses the importance of thermodynamic composition fluctuations in creating and determining the unique local environment experienced by each component [14, 15, 16, 17, 18]. The third approach postulates that the relevant length-

scale for the determination of local composition is the Kuhn length [19], and that within this region the composition will be biased by the effects of chain connectivity [19, 20, 21, 22]. This chain-connectivity approach has recently been shown to capture much of the composition and temperature dependence of miscible blend dynamics [23, 24, 25, 26].

From a model-independent perspective, the local composition surrounding a relaxing polymer segment can be conveniently subdivided into intermolecular and intramolecular contributions. In a miscible A/B blend, intermolecular contributions provide both A and B segments to the local composition. The intramolecular contributions to the local composition surrounding an A segment only add other A segments. It would be useful to isolate the intermolecular and intramolecular effects on blend dynamics; tracer blends are helpful to this end. In a blend consisting of a dilute A tracer in a pure B matrix the local composition of A segments surrounding the tracer are due solely to intramolecular contributions. Does the time-temperature superposition principle hold, as in homopolymers, or does it fail, as in blends with intermediate compositions? The success or failure of time-temperature superposition has implications regarding the role of intermolecular A-A contacts in producing thermorheological complexity: successful superposition could indicate that intermolecular effects are decisive, whereas failure implies that intermolecular contributions to the local composition are not required to produce "dynamic heterogeneity". In this way, tracer blends provide an additional test of blend dynamics models. In this paper, we assess time-temperature superposition for blends consisting of a small fraction of polyisoprene (PI) in a poly(vinyl ethylene) (PVE) matrix and a small fraction of PVE in a PI matrix. Dynamic viscosity measurements were made on PVE in PI and PI in PVE tracer blends. In the former, the dynamics of the PVE tracer could be extracted clearly, and the data were compared with the predictions of the model of Lodge and McLeish.

Materials and methods

Materials synthesis and characterization The two PI samples (PI-5 and PI-78) and the two PVE samples (PVE-5 and PVE-120) were synthesized via anionic polymerization; the numerical designation corresponds to the number-average molecular weight in kilograms/mole. The synthesis and characterization of PI-78 and PVE-120 have been described elsewhere [25]. The PI-5 and PVE-5 samples were provided by N. Lynd and Z. Zhou, respectively. All of these polymers are hydroxyl terminated, which facilitates subsequent labeling with a photochromic dye for tracer diffusion measurements by forced Rayleigh scattering. The polymer molecular weights and molecular weight distributions were determined by size exclusion chromatography, and the microstructures were determined by ^{1}H NMR. The characteristics of the four polymers are summarized in Table 1. Blends were prepared by codissolving polymers in methylene chloride with 0.5% by weight 2,6-di-*tert*-butyl-4-methyl-phenol (antioxidant). The solvent was evaporated under nitrogen, and the samples were annealed under vacuum at 70 °C for 12 h. All blend compositions are reported in percent by weight.

Rheology Dynamic viscosity measurements were made with an ARES rheometer (Rheometric Scientific) using 25 mm parallel plates. Gap spacings of approximately 1 mm were employed for all measurements. The gap was adjusted at each temperature and a thermal expansion correction of 2.4 μm/°C was applied in order to determine the gap width. Measurements were made at temperatures ranging from –20 °C to 60 °C. The sample and toolset were enclosed in a nitrogen convection oven; at all times the sample temperature was maintained within ±0.5 °C of the set point. Measurements of the complex viscosity (η^*) as a function of frequency (ω) were carried out in the linear viscoelastic regime.

Results and discussion

$\eta^*(\omega)$ was measured for four samples: PI-5 homopolymer, PVE-5 homopolymer, a blend of 1% PVE-120/99% PI-5, and a blend of 1% PI-78/99% PVE-5. The component of η^* in phase with the rate of strain (η') and the phase angle (δ) are plotted in Fig. 1 for PI-5 and the 1% PVE-120/99% PI-5 blend at selected temperatures. At all temperatures, the magnitude of η' was greater for the tracer blend than it was for the pure PI matrix. This difference reflects the increase in viscosity due to the addition of a small amount of high molecular weight, higher T_g material (PVE-120) to a low molecular weight, lower T_g matrix (PI-5). The difference between blend and matrix viscosities increased as the measurement temperature decreased. It should also be noted that the presence of the tracer PVE has a significant effect on δ. For the pure PI-5 matrix polymer, δ is approximately 90° over most of the frequency range examined, consistent with a purely viscous response. The addition of

Table 1 Characteristics of PI and PVE homopolymers

Sample	M_n (kg/mol)	M_w/M_n	Microstructure	
			1,4	3,4
PI-5	5.5	1.01	93%	7%
PI-78	78	1.02	95%	5%
			1,2	1,4
PVE-5	5.3	1.05	95%	5%
PVE-120	120	1.01	95%	5%

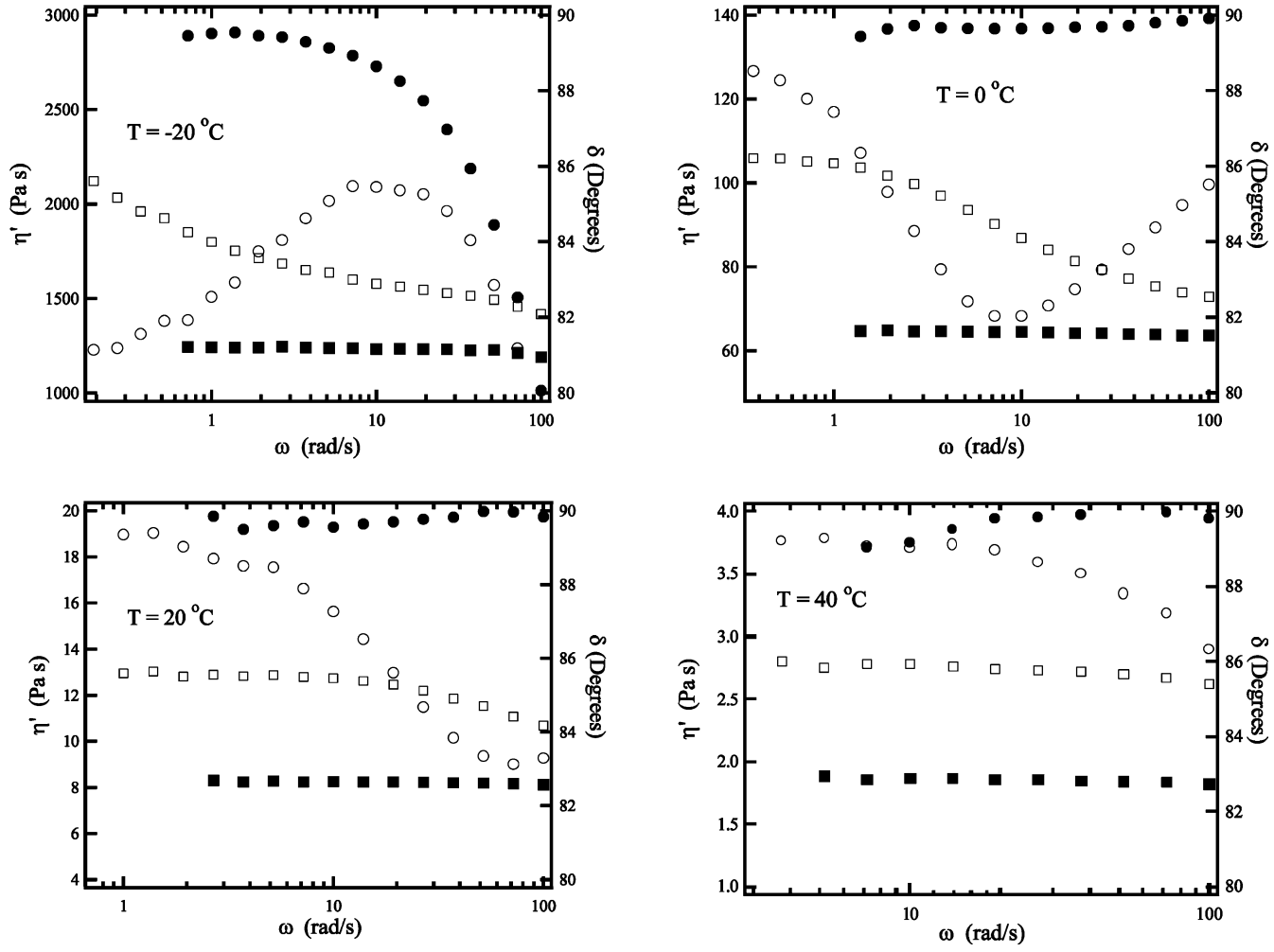

Fig. 1 Dynamic viscosity results for polyisoprene (PI)-5 and 1% poly(vinyl ethylene) (PVE)-120/99% PI-5 at selected temperatures. Viscosity (η') for PI-5 (*black squares*) and for 1% PVE-120/99% PI-5 (*white squares*), and phase angle (δ) for PI-5 (*black circles*) and for 1% PVE-120/99% PI-5 (*white circles*) are plotted

the tracer PVE to the PI matrix brings about a clear change in δ, suggesting that it should be possible to isolate the contribution of the PVE tracer to the macroscopic rheological response of the blend.

The η' and δ results for PVE-5 and the 1% PI-78/99% PVE-5 blend are presented for selected temperatures in Fig. 2. The magnitude of η' for the blend was greater than for the PVE-5 matrix, but the extent of this difference was much less than observed for the PVE tracer blend. At temperatures below 30 °C, the frequency dependences of δ for the blend and PVE-5 samples are almost identical. This suggests that below 30 °C the PVE matrix is dominating the frequency dependence of the viscoelastic response of the blend. Above 30 °C, δ of PVE-5 has almost no frequency dependence, and the dependence of δ in the blend is likely due to the dynamics of the PI tracer. These observations on the PI tracer blend have consequences for the time-temperature superposition analysis reported in the next section.

Time-temperature superposition and comparison of component dynamics

Time-temperature superposition was attempted on the two tracer blends. The apparent shift factor (a_T) for each temperature was determined by attempting to superpose tan(δ) versus ω plots for different temperatures. The "best" superpositions are shown in Fig. 3a and Fig. 3b for the PVE tracer blend and the PI tracer blend, respectively. In Fig. 3a the failure of time-temperature superposition is evident in the a_T ω range of 10^3–10^5 rad/s. The scatter in tan(δ) at low values of $a_T\omega$ is due to the experimental difficulty of resolving the phase angle as the rheological response of the material becomes increasingly viscous in nature. This generally occurs as tan(δ) nears a value of 100. This phase angle resolution problem generally cannot be overcome by

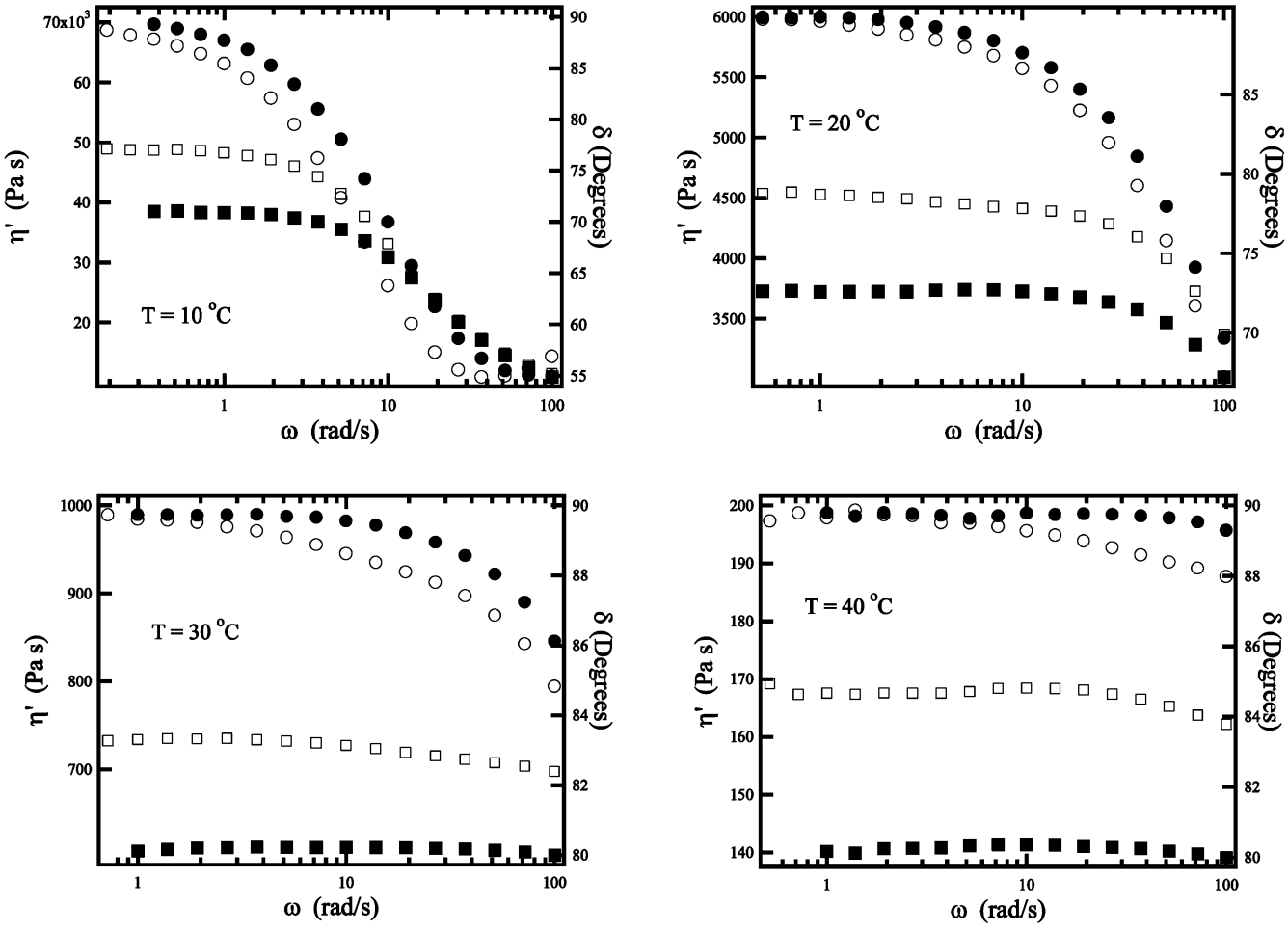

Fig. 2 Dynamic viscosity results for PVE-5 and 1% PI-78/99% PVE-5 at selected temperatures. η' for PVE-5 (*black squares*) and for 1% PI-78/99% PVE-5 (*white squares*), and δ for PVE-5 (*black circles*) and for 1% PI-78/99% PVE-5 (*white circles*) are plotted

increasing strain amplitude. In Fig. 3b, time-temperature superposition failure occurs in the $a_T\ \omega$ range of 10^2–10^4 rad/s. For the PI tracer blend in Fig. 3b, the failure is most pronounced when comparing data at 20 °C and 30 °C; at temperatures above approximately 30 °C the PI tracer begins to dominate the frequency response of δ as discussed above, whereas below 30 °C the PVE matrix controls the frequency response of δ.

Extraction of monomeric friction factor from tracer rheology experiment

The contribution of the PVE tracer to $\eta^*(\omega)$ of the 1% PVE-120/99% PI-5 blend was extracted in order to allow for a quantitative comparison of the temperature dependence of the dynamics of each blend component. The blend was assumed to be unentangled (i.e. Rouse-like), and thus $\eta^*(\omega)$ of the blend can be described by:

$$\eta^*_{\text{blend}}(\omega) = w_{\text{PVE}}\eta^*_{\text{PVE}}(\omega) + w_{\text{PI}}\eta^*_{\text{PI}}(\omega) \quad (1)$$

where w_{PVE} and w_{PI} are the weight fractions of PVE and PI, respectively. This is similar to the analysis of a dilute polymer solution, where in this case the "solvent" is the PI-5 matrix, which has some viscoelasticity at low temperatures. Both $\eta^*_{\text{blend}}(\omega)$ and $\eta^*_{\text{PI}}(\omega)$ were experimentally measured, so the application of Eq. 1 to extract $\eta^*_{\text{PVE}}(\omega)$ is straightforward. This approach was not as successful for extracting the PI tracer dynamics from the 1% PI-78/99% PVE-5 blend, as the contribution of PI-78 to $\eta^*_{\text{blend}}(\omega)$ is relatively small, and thus the extracted $\eta^*_{\text{PI}}(\omega)$ contains an unacceptably high level of noise.

A master curve for $\eta^*_{\text{PVE}}(\omega)$ from the 1% PVE-120/99% PI-5 blend was created via time-temperature superposition. A plot of tan(δ) versus $a_T\ \omega$ for the PVE tracer contribution to the blend is shown in Fig. 4; as can be seen, time-temperature superposition is successful for $\eta^*_{\text{PVE}}(\omega)$. This allows for the determination of a_T as a function of temperature for the PVE tracer in the blend. These shift factors for the PVE tracer are plotted in Fig. 5, along with the shift factors for PI-5 that were determined via time-temperature superposition of the PI-5

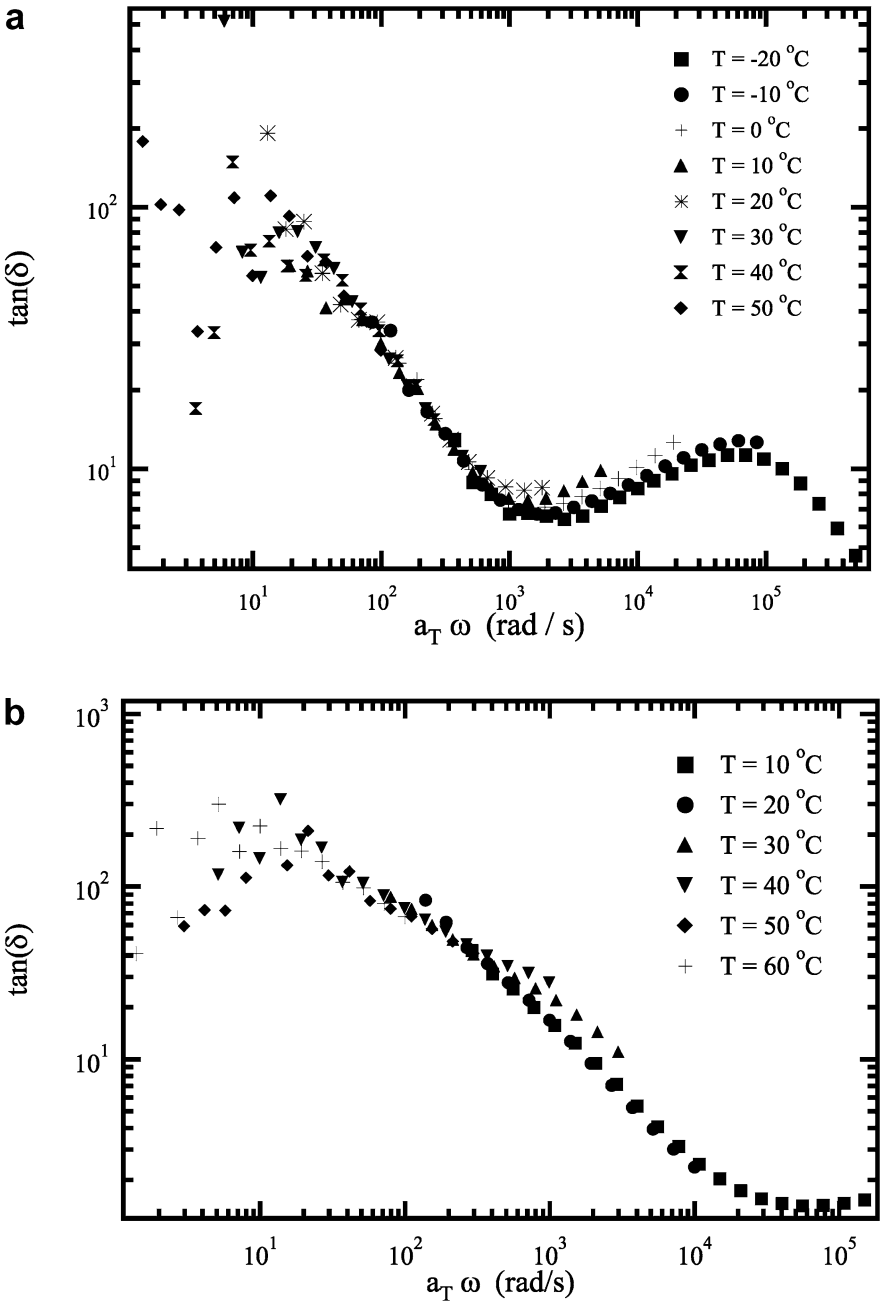

Fig. 3a, b Time-temperature superposition analysis for tracer blends. tan(δ) vs apparent $a_T\omega$ is plotted **a** for 1% PVE-120/99% PI-5, and **b** for 1% PI-78/99% PVE-5 at selected temperatures

homopolymer measurements (not shown). Both components were shifted to a common reference temperature of 50 °C. At –20 °C, the PVE shift factor is a factor of approximately 2.5 greater than the PI shift factor. This result is consistent with, and quantifies the time-temperature superposition failure presented in Fig. 3a.

Monomeric friction factors (ζ) can be extracted for PVE from the tracer rheology experiment in the following manner. For higher temperature measurements, in this case $T > 0$ °C, the zero shear viscosity (η_o) can be extracted by taking the value of $\eta'_{PVE}(\omega)$ in the limit $\omega \to 0$. For lower temperature data, where the low frequency limiting value of $\eta'_{PVE}(\omega)$ cannot be observed, η_o can be determined by the relationship:

$$\eta_o(T) = \frac{a_T(T)}{a_T(T_{ref})}\eta_o(T_{ref}) \quad (2)$$

where T_{ref} is a reference temperature where η_o can be reliably determined. We have omitted the contribution of the vertical shift factor b_T in Eq. 2, as it is generally a weak function of temperature, and has at most a very modest effect on the value of η_o. In order to determine ζ

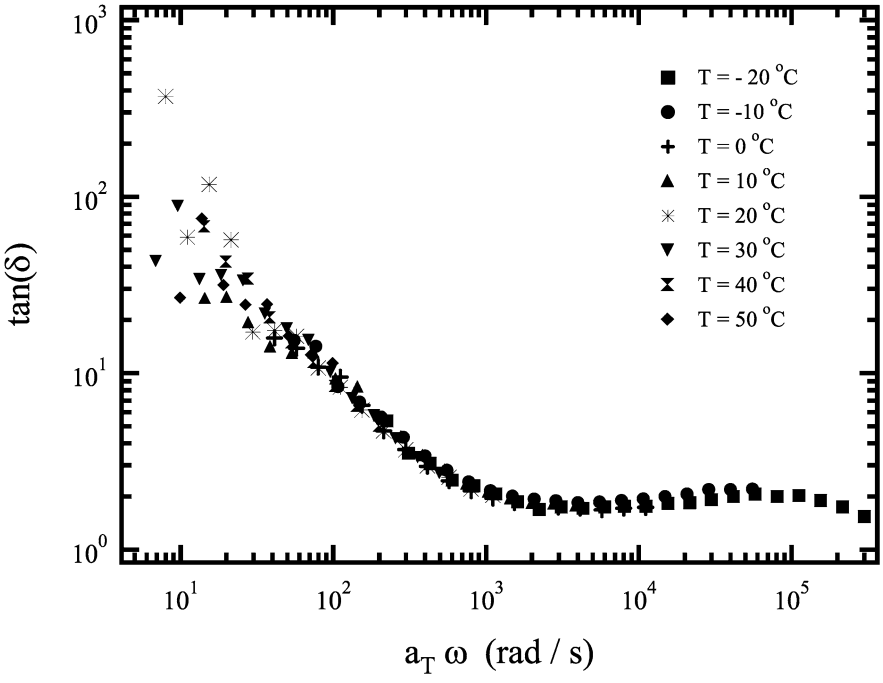

Fig. 4 Time-temperature superposition analysis for extracted PVE-120 tracer contribution. tan(δ) vs a_T ω is plotted for the PVE-120 tracer contribution to dynamic viscosity at selected temperatures

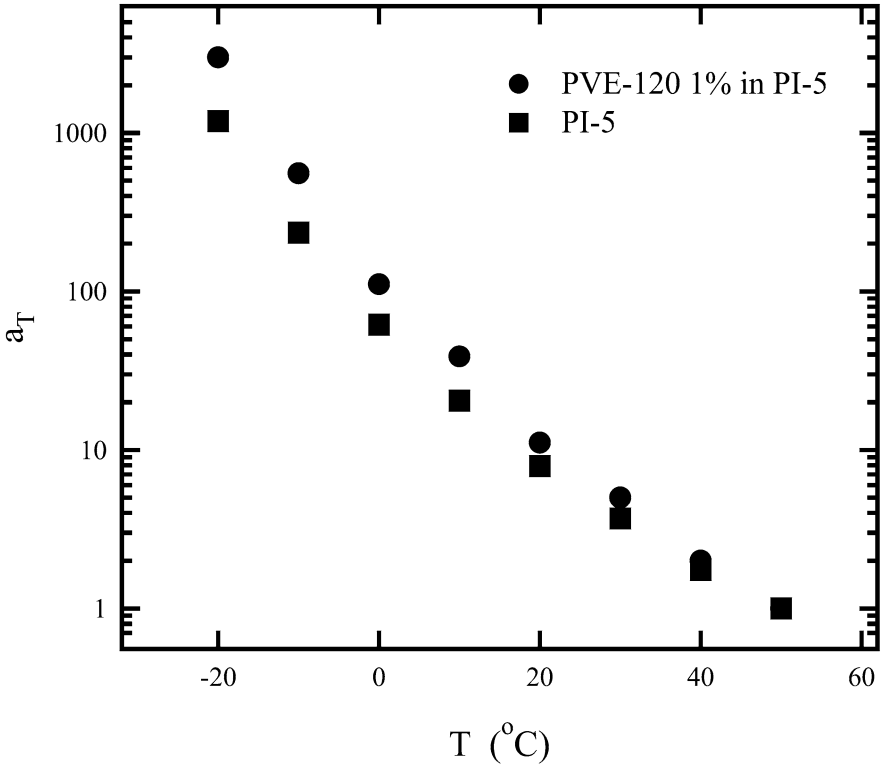

Fig. 5 Shift factors as a function of temperature for the PI-5 matrix and the extracted PVE-120 tracer of the 1% PVE-120/99% PI-5 blend

from η_o, the Rouse model was assumed to govern the dynamics of the PVE tracer chain, and thus the relation between ζ and η_o is [27, 28]:

$$\eta_o = \frac{1}{36}\rho N_{av} b^2 \zeta \frac{M}{M_o} \quad (3)$$

where ρ is the density, N_{av} is Avogadro's number, b is the polymer statistical segment length, M is the molecular weight, and M_o is the molecular weight of a repeat unit. The extracted values of ζ are plotted in Fig. 6 as a function of temperature.

Significance of time-temperature superposition failure for tracer blends

The time-temperature superposition failure for the two tracer blends suggests that each blend component retains a distinct and separate temperature dependence even at the dilute tracer compositions examined. This, in turn, indicates that intramolecular contributions to local composition, such as self-concentration, combined with intrinsic differences in component dynamics are sufficient to cause time-temperature superposition failure.

Recent dynamic Monte Carlo simulation results have examined a similar tracer blend scenario [29]. In the simulation, the diffusion coefficient of a high T_g polymer tracer had a different temperature dependence from the low T_g polymer matrix, in qualitative agreement with the time-temperature superposition failure reported above for PVE tracer in PI matrix. In the same simulation study, the diffusion coefficient of the low T_g polymer had the same temperature dependence as the high T_g matrix [29], a conclusion which is at odds with the time-temperature superposition failure observed here for the PI tracer in PVE matrix. The authors of the simulation study found that the low T_g (faster) polymer had to wait until the higher T_g (slower) polymer moved and opened up space for a subsequent relaxation of the faster polymer [29]. This is a sensible explanation of the Monte Carlo simulation results, where the length-scale of motion is related to and fixed by the lattice spacing, and other monomers that reside within this length-scale will have to move out of the way in order to make room for local motion. These neighboring monomers are mostly from the slower moving component, and therefore the motion of these slower moving monomers becomes the rate-limiting step in the relaxation of the faster moving monomers. In an experimental situation, the length-scale and mechanism of local motion remains unclear, though the experimental results presented here and published elsewhere [30] imply that the motion of the faster moving tracer component in a blend is not constrained so much by the slower moving component that the two components' dynamics have the same temperature dependence.

Comparison of ζ with the Lodge-McLeish model

The model of Lodge and McLeish (L-M) [19] has recently been shown to be successful in capturing some aspects of the dynamics of miscible polymer blends [23, 24, 25, 26]. Here, we briefly recap the implementation of the L-M model and compare it to the experimental measurements of ζ in PVE tracer blend.

The primary postulate of the L-M model is that the local relaxations that determine ζ are influenced by the mean composition within a Kuhn length (ℓ_k) of the relaxing segment. The volume (V) of this region is taken to be $V \approx \ell_k^3$. Due to chain connectivity, a certain fraction of V must be occupied by neighboring monomers from the same chain as the relaxing segment. Thus, the composition in V is different from the macroscopic blend composition (ϕ), and the relaxing segment senses a composition that is enriched in itself. This effective local

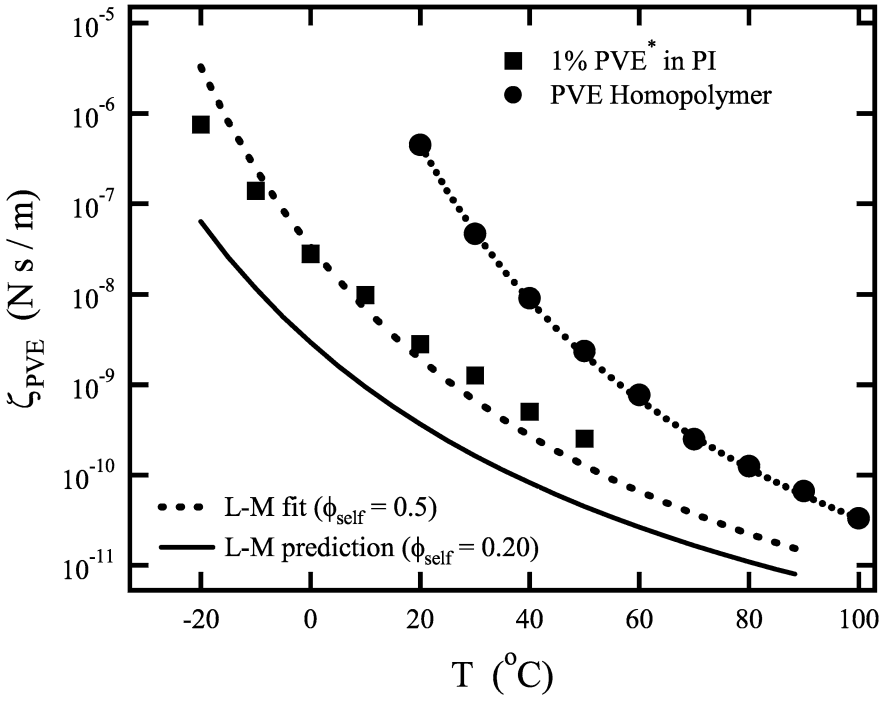

Fig. 6 Comparison of extracted $\zeta(T)$ for PVE-120 tracer to the Lodge and McLeish (*L-M*) model. Also plotted is monomeric friction factor [$\zeta(T)$] for PVE-120 homopolymer from [24]. The dotted line through the homopolymer data represents a Williams-Landel-Ferry fit with the parameters $C_1^g = 10.86$, $C_2^g = 50$ °C, $\zeta_g = 0.571$ dyn s/cm, and $T_g = 0$ °C

composition for blend component A ($\phi_{\mathrm{eff,A}}$), is calculated by [19]:

$$\phi_{\mathrm{eff,A}} = \phi_{\mathrm{s,A}} + \left(1 - \phi_{\mathrm{s,A}}\right)\phi \tag{4}$$

where $\phi_{\mathrm{s,A}}$ is the "self-concentration" for component A. $\phi_{\mathrm{s,A}}$ is simply the fraction of a region of size V that is occupied by a Kuhn length's worth of monomers [19]:

$$\phi_{\mathrm{s}} = \frac{C_{\infty} M_{\mathrm{o}}}{n \rho N_{\mathrm{av}} V} \tag{5}$$

where C_{∞} is the characteristic ratio and n is number of backbone bonds per repeat unit. As noted previously, Eq. 5 could also contain a prefactor of order unity, as the definition $V = \ell_{\mathrm{k}}^3$ is somewhat arbitrary [19].

In order to calculate ζ, two additional steps are necessary. The Fox equation is used to calculate an effective glass transition temperature ($T_{\mathrm{g,eff}}$) from ϕ_{eff}:

$$\frac{1}{T_{\mathrm{g,eff}}} = \frac{\phi_{\mathrm{eff}}}{T_{\mathrm{g,A}}} + \frac{1 - \phi_{\mathrm{eff}}}{T_{\mathrm{g,B}}} \tag{6}$$

where $T_{\mathrm{g,A}}$ and $T_{\mathrm{g,B}}$ are the glass transition temperatures of polymers A and B. The final step in the calculation of ζ is to use the Williams-Landel-Ferry (WLF) relationship [31]:

$$\log\left(\frac{\zeta(\phi, T)}{\zeta_{\mathrm{g}}}\right) = \frac{-C_1\left[T - T_{\mathrm{g,eff}}(\phi)\right]}{C_2 + T - T_{\mathrm{g,eff}}(\phi)} \tag{7}$$

where ζ_{g},C_1, and C_2 are WLF parameters for the polymer component that are assumed to be independent of composition. This general approach has recently been shown to describe the temperature and composition dependence of PI dynamics in PI/PVE blends in a near quantitative manner and to capture the major trends in the temperature and composition dependence of PVE in PI/PVE blends [25].

In Fig. 6, a comparison is made between the experiment and the L-M prediction for $\zeta(T)$ for a PVE tracer in a PI matrix. Also plotted for reference in Fig. 6 is the experimentally determined $\zeta(T)$ for PVE homopolymer. The solid line represents the L-M prediction using $\phi_{\mathrm{s,PVE}} = 0.2$, as has been suggested by previous measurements [25]. With this self-concentration value the L-M model underpredicts the value of ζ for the PVE tracer by roughly an order of magnitude. The dashed line in Fig. 6 represents a best fit of the L-M model to the experimental data, using $\phi_{\mathrm{s,PVE}} = 0.5$. While better agreement between theory and experiment occurs in this case, the L-M fit still does not have the same temperature dependence as the experimental data.

We note that in Fig. 6 the L-M prediction that employs $\phi_{\mathrm{s,PVE}} = 0.2$ (corresponding to a self-concentration length-scale approximately equal to the Kuhn length) overpredicts the effects of blending with PI when compared with experimental data. This result is important, because it suggests that the self-concentration effect predicted by the L-M model is not strong enough to account for the tracer dynamics of PVE in a PI matrix. In other words, in the framework of the L-M model, the results in Fig. 6 suggest that the length-scale for self-concentration for PVE in the tracer limit is significantly less that the Kuhn length. From Eq. 5, the length-scale is estimated to be approximately 8 Å, less than the 12 Å value that was previously extracted [25].

Conclusions

We have reported the measurement of dynamic viscosity for blends consisting of a tracer of PI in a PVE matrix and a tracer of PVE in a PI matrix. Time-temperature superposition failure was observed for both of the tracer blends. The monomeric friction factor of the PVE tracer was extracted and compared to the model of Lodge and McLeish. The predictions of the L-M model using the expected value of self-concentration underestimated the tracer monomeric friction factor by roughly an order of magnitude. A best-fit value of self-concentration was obtained. The central results of this paper are:

-1. In PI/PVE blends at the extremes of composition (i.e. tracer blends) the dynamics of a particular component retain a unique temperature dependence, distinct from that of the other blend component.
-2. This result indicates that the net contribution of like segments to the local environment of a test segment is dominated by intramolecular effects. By extension, long-range concentration fluctuations are not necessary to observe superposition failure.
-3. The self-concentration effect for a PVE tracer in a PI matrix is significantly stronger than anticipated by the L-M model, suggesting that the relevant length-scale may be even shorter than the Kuhn length in this case.

Acknowledgements This work was supported by the National Science Foundation, through Award No. DMR-9901087. We would like to thank N. Lynd and Z. Zhou for providing the PI-5 and PVE-5 samples, and M. D. Ediger for helpful discussions.

References

1. Minnick MG, Schrag JL (1980) Macromolecules 13:1690
2. Colby RH (1989) Polymer 30:1275
3. Roovers J, Toporowski PM (1992) Macromolecules 25:1096
4. Roovers J, Toporowski PM (1992) Macromolecules 25:3454
5. Pathak JA, Colby RH, Floudas G, Jerome R (1999) Macromolecules 32:2553
6. Trask CA, Roland CM (1989) Macromolecules 22:256
7. Composto RJ, Kramer EJ, White DM (1990) Polymer 31:2320
8. Green PF, Adolf DB, Gilliom LR (1991) Macromolecules 24:3377
9. Kim E, Kramer EJ, Osby JO (1995) Macromolecules 28:1979
10. Miller JB, McGrath KJ, Roland CM, Trask CA, Garroway AN (1990) Macromolecules 23:4543
11. Ngai KL, Rendell RW, Rajagopal AK, Teitler S (1986) Ann N Y Acad Sci 484:150
12. Roland CM, Ngai KL (1991) Macromolecules 24:2261
13. Roland CM, Ngai KL (1992) J Rheol 36:1691
14. Katana G, Fischer EW, Hack T, Abetz V, Kremer F (1995) Macromolecules 28:2714
15. Zetsche A, Fischer EW (1994) Acta Polym 45:168
16. Kumar SK, Colby RH, Anastasiadis SH, Fytas G (1996) J Chem Phys105:3777
17. Kamath S, Colby RH, Kumar SK, Karatasos K, Floudas G, Fytas G, Roovers JEL (1999) J Chem Phys111:6121
18. Salaniwal S, Kant R, Colby RH, Kumar SK (2002) Macromolecules 35:9211
19. Lodge TP, McLeish TCB (2000) Macromolecules 33:5278
20. Lau SF, Pathak J, Wunderlich B (1982) Macromolecules 15:1278
21. Chung GC, Kornfield JA, Smith SD (1994) Macromolecules 27:964
22. Gell CB, Krishnamoorti R, Kim E, Graessley WW, Fetters LJ (1997) Rheol Acta 36:217
23. Leroy E, Alegria A, Colmenero J (2002) Macromolecules 35:5587
24. Hirose Y, Urakawa O, Adachi K (2003) Macromolecules 36:3699
25. Haley JC, Lodge TP, He Y, Ediger MD, Von Meerwall ED, Mijovic J (2003) Macromolecules 36:6142
26. He Y, Lutz TR, Ediger MD (2003) J Chem Phys 119:9956
27. Rouse PE (1953) J Chem Phys 21:1272
28. Doi M, Edwards SF (1986) The theory of polymer dynamics. Oxford University Press, Oxford
29. Kamath S, Colby RH, Kumar SK (2003) Macromolecules 36:8567
30. Lutz TR, He Y, Ediger MD, Cao H, Lin G, Jones AA (2003) Macromolecules 36:1724
31. Ferry, JD (1980) Viscoelastic properties of polymers. Wiley, New York